

Available online at www.sciencedirect.com

ScienceDirect

journal homepage: www.keaipublishing.com/jtte

Original research paper

Machine detectability of road markings analysed with classical image processing techniques towards demand-oriented road operations for automated vehicles

Stefan Biermeier^a, Dirk Kemper^a, Tomasz E. Burghardt^b,
Alvaro Garcia-Hernandez^{a,*}

^a Lehrstuhl und Institut für Straßenwesen, RWTH Aachen University, Aachen 52074, Germany

^b M. Swarovski Gesellschaft m.b.H., Wipark, 14. Straße 11, Neufurth 3363, Austria

HIGHLIGHTS

- A multi-parameter approach is proposed to assess machine detectability (MD) of road markings.
- Retroreflectivity predicts MD under certain conditions; diffuse light is less effective.
- Findings emphasise the importance of assessing MD across diverse driving conditions.
- Insights support the development of demand-oriented standards for road markings.

ARTICLE INFO

Article history:

Received 21 March 2024

Received in revised form

29 October 2024

Accepted 14 November 2024

Available online 4 June 2025

Keywords:

Automated driving systems

Operational design domain

Physical infrastructure

Lane keeping system

Weather conditions

Multi-parameter approach

ABSTRACT

This paper investigates the machine detectability (MD) of road markings under various environmental conditions, crucial for the definition of operational design domains (ODD) of automated driving systems as well as the assessment of operational domains (OD). By analysing the correlation between MD parameters, specifically contrast, gradient, and edge detectability, and common photometric properties of road markings currently used for maintenance management (retroreflectivity and daytime visibility), the paper aims to bridge the gap in current road marking detectability research and OD assessment. The methodology encompassed a detailed examination of road markings on a motorway under different lighting and weather conditions, employing both camera and LiDAR sensors for data collection. The findings reveal that the retroreflectivity is a consistent predictor for MD in camera images during nighttime and for LiDAR contrast in dry and moist conditions, whereas the daytime visibility fails to reliably predict MD in daytime conditions. Moreover, the study introduces a multi-parameter approach that transcends sole contrast analysis as well as the usage of off-the-shelf machine vision systems, proposing a new set of MD parameters for a broader and transparent evaluation of road marking detectability. This comprehensive assessment highlights the need for quality standards for road markings that would accommodate varying environmental impacts on MD of road markings.

* Corresponding author.

E-mail addresses: biermeier@isac.rwth-aachen.de (S. Biermeier), tomasz.burghardt@swarco.com (T.E. Burghardt), alvaro@isac.rwth-aachen.de (A. Garcia-Hernandez).

Peer review under responsibility of Chang'an University

<https://doi.org/10.1016/j.jtte.2024.11.003>

2095-7564/© 2025 Chang'an University. Publishing services by Elsevier B.V. on behalf of KeAi Communications Co. Ltd. This is an open access article under the CC BY-NC-ND license (<http://creativecommons.org/licenses/by-nc-nd/4.0/>).

Ultimately, this research provides valuable insights and recommendations on research approaches to find demand-oriented minimum standards for MD of road markings, enabling comprehensive OD assessments, and facilitating safer navigation for automated vehicles.

1. Introduction

Road markings significantly contribute to safe traffic guidance (Calvi, 2014; Carlson et al., 2013; Han et al., 2023). They may indicate lanes or other rules of traffic. Not only human drivers use the information road markings are providing. Their consistent presence at almost all roads has also led to their adoption as a guidance system for automated vehicles (Yang et al., 2023).

In terms of highly automated driving systems, operational design domains (ODD) define theoretical ranges of driving conditions for which a specific automated driving system is designed to operate in. In contrast, operational domains (OD) describe the actual road and its conditions for which an automated system applies for an authorisation to operate. When matching ODD to specific OD in approval procedures for highly automated vehicles, assessing the condition of physical infrastructure like road markings plays an important role (Pappalardo et al., 2022). To detect and recognise road markings, automated vehicles use sensors, such as cameras or light detection and ranging (LiDAR), which capture and process the images or point clouds of the road scene (Katzorke et al., 2022; Muckenhuber et al., 2021; Yeong et al., 2021).

As it is true for every detection task, the quality of signal processing results and the benefits in terms of existing and further vehicle functions not only depend on the quality of the sensor and signal processing but also on machine detectability (MD) of road marking. In this paper, MD is understood as the manifestation of physical and photometric properties of road markings on the expression of features that are extracted and used to classify image segments or objects in sensor data.

Road markings are physical entities with measurable photometric properties, not just digital representations. These properties are described by the coefficient of retroreflected luminance R_L (mcd/lx/m²) and the luminance coefficient in diffuse illumination Q_d (mcd/lx/m²). Q_d measures diffuse transmitted light reflected from a horizontal surface to the position of a driver, while R_L measures retroreflective quality for nighttime visibility (Brémond, 2019). To fit photometric requirements, certain material properties can be adjusted. Road marking systems are composed of different materials and subproducts. Common materials include paints, non-prefabricated cold and hot plastics, and prefabricated tapes in white, yellow, or orange colours, allowing for better detection on darker surfaces or differentiation from differently coloured markings. To ensure headlight retroreflection, glass or ceramic beads are integrated in the plastics surface (Pocock and Rhodes, 1952). Macrotecture can

be added to the plastics and tapes to ensure drainage and thus preserve retroreflection in wet conditions (Schnell et al., 2003). However, road markings are subject to wear and degradation over time due to traffic loads, making it crucial to monitor their properties on the road and ensure minimum quality standards (Burghardt et al., 2021a; Wenzel et al., 2022).

The current monitoring practices utilise photometric systems to evaluate the functional characteristics relevant to human driver requirements. This raises the question of whether the existing measurements enable us to infer the MD property of road markings, given the potential disparities between sensor-based detection and human perception. Similar concerns arise when establishing minimum standards.

Previous studies on the detection of road markings in camera images or LiDAR point clouds have focused on different aspects of markings, such as retroreflectivity, line width, contrast ratio, clarity, and uniformity (Burghardt et al., 2020). Some studies have been conducted on public roads (Babić et al., 2021; Li et al., 2021; Pappalardo et al., 2021, 2022; Pike et al., 2018a; Storsæter et al., 2021a), while others have taken place in controlled environments like laboratories and closed test tracks (Burghardt et al., 2021b, 2023; Marr et al., 2020; Pike et al., 2018b, 2019; Storsæter et al., 2021b). These studies have investigated not only dry surfaces but also wet surfaces (Burghardt et al., 2023; Marr et al., 2020; Pike et al., 2018b, 2019), rainy or foggy conditions (Burghardt et al., 2021b; Storsæter et al., 2021a), backlight and glare (Burghardt et al., 2023; Marr et al., 2020; Pike et al., 2018b, 2019), or even snow (Storsæter et al., 2021b). However, most of the studies conducted so far utilised black box machine vision systems, off-the-shelf, or machine learning methods. Moreover, some of the studies have used basic classical machine vision techniques, but only in laboratory settings (Burghardt et al., 2023; Pike et al., 2019; Storsæter et al., 2021b).

A major drawback of off-the-shelf machine vision systems is that they do not reveal the specific image features that enable them to detect road markings. This lack of transparency leads to inconsistent findings and recommendations (Pike et al., 2018a) and adds complexity to assessing MD of road markings. Therefore, as suggested in Marr et al. (2020), a more detailed understanding of road marking detectability is needed.

Using classical machine vision techniques and image processing methods offer the possibility for transparent and differentiated evaluation to accurately quantify MD properties. For objects with lower feature complexity, such as longitudinal road markings, feature learning and feature engineering yield comparable results (O'Mahony et al., 2019). Lim and Braunl (2019) provided a comprehensive overview

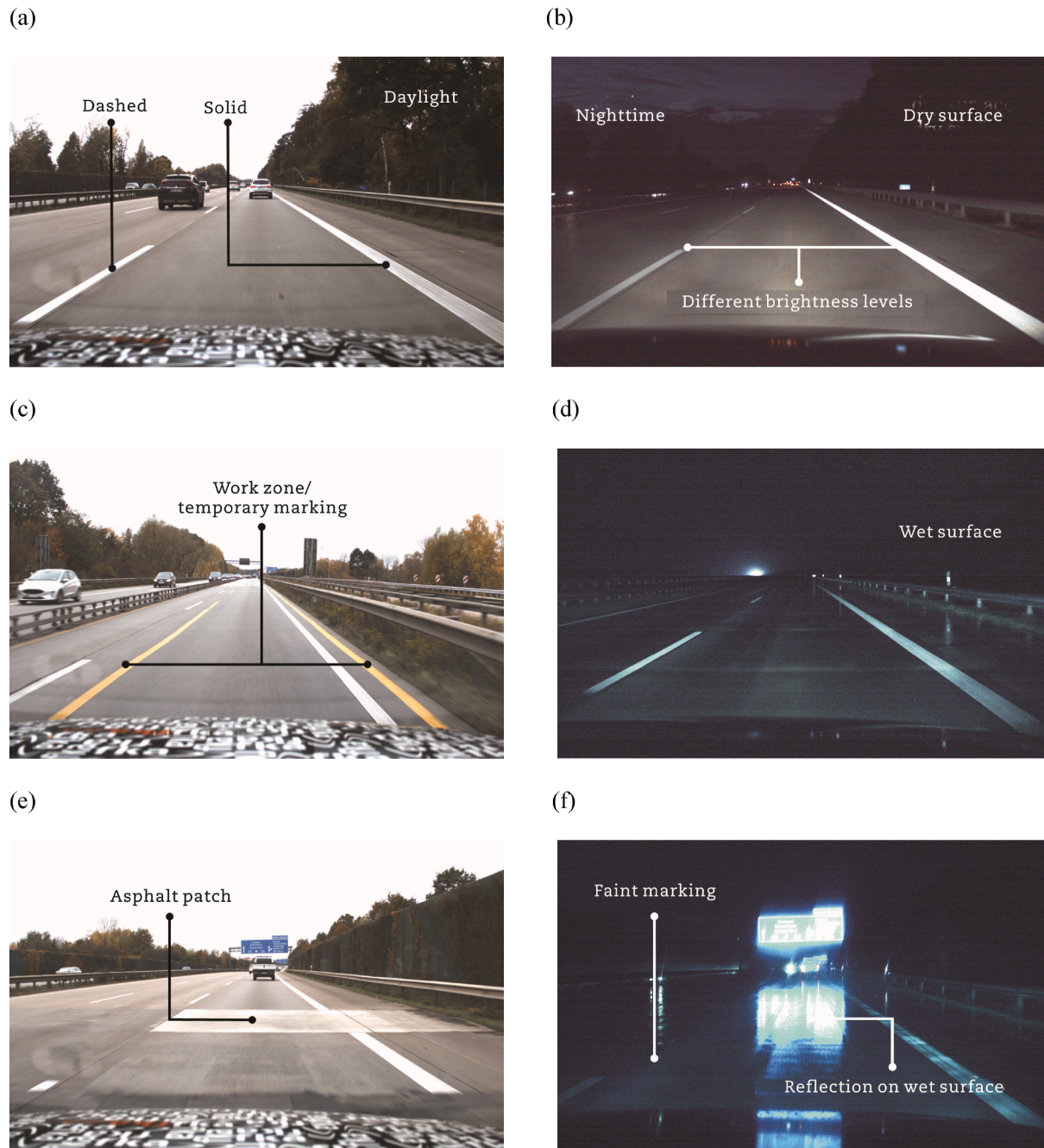


Fig. 1 – Examples of the road surfaces examined. (a) Dashed and solid markings. (b) Nighttime conditions. (c) Work zones with temporary yellow markings. (d) Wet surface conditions. (e) High-contrast asphalt patches. (f) Wet surfaces at night with traffic sign reflections and faint markings.

of conventional methods, learning methods, and practical implementations for road space detection. Veit et al. (2008) discussed longitudinal markings in particular.

This paper aims to address the gap in the research of road marking detectability and propose a transparent signal processing metric to determine MD of road markings. This metric includes a new set of MD parameters that evaluate the input quality for common feature extraction methods, such as thresholding, edge detection, and ridge detection.

This metric will be used to investigate two research questions related to the MD of road markings.

- (1) Can a correlation be established between MD parameters and common photometric road markings parameters, i.e., retroreflectivity (R_L) and daytime visibility (Q_d)?
- (2) Is a multi-MD-parameter approach necessary to reveal effects on the MD of road markings that cannot be described by sole image contrast analysis?

Table 1 – Road markings classification.

Name	Macrotexture	Property	Comment
D1	<2 mm (flat)	White tape, width: 15 cm, dashed	The original tape product featured an approx. 2 mm macrostructure, worn down to 0.5–1.5 mm due to traffic. The material was uniformly applied without intended macrotexture. The underlying road surface imparts a minimal macrostructure of 0.5–1.5 mm. Material was irregularly distributed. The macrostructure was between 2.5 and 4.0 mm.
D2		White cold spray plastic, width: 15 cm, dashed line	
D3			
D4	>2 mm (structured)	White cold plastic agglomerates, width: 15 cm, dashed line	
D5			The original tape product featured an approx. 2 mm macrostructure, worn down to 0.5–1.5 mm due to traffic. Materials were irregularly distributed. The macrostructure was between 2.5 and 4.0 mm.
D6			
D7		White tape, width: 30 cm, solid line	
S1	<2 mm (flat)		
S2			Materials were irregularly distributed. The macrostructure was between 2.5 and 4.0 mm.
S3			
S4	>2 mm (structured)	White cold plastic, agglomerates, width: 30 cm, solid line	
S5			
S6			Materials were irregularly distributed. The macrostructure was between 2.5 and 4.0 mm.
S7			
W1	<2 mm (flat)	Yellow tape, width: 15 cm, solid line	
W2			
W3			The original yellow tapes product examined did not have macrotexture.
W4			
W2	<2 mm (flat)	Yellow tape, width: 15 cm, solid/broken line	

Addressing these questions through experimental data collected from a public road under various lighting and weather conditions will provide insights on whether common photometric properties are suitable measures to describe the MD of road markings. Furthermore, the study aims to offer recommendations for the most relevant image features for road marking detection.

2. Methodology

2.1. Road and road markings examined

The study examined road markings on nine 100 m segments of a German motorway's right lanes (3.75 m wide), selected for varied materials that include cold spray plastic, tape, and cold plastic agglomerates, and diverse states and styles such as solid, dashed, worn, and work zone markings, along with patched areas. Road geometry wise, the segments have limited curvature, ensuring consistent viewing angles across all segments. Observations were made in varying conditions including wet, dry, and different lighting. Fig. 1 shows additional details.

To differentiate the road markings, they have been labelled in this paper as S for solid stripes, D for dashed stripes, and W for temporary markings in work zones. Table 1 shows additional information on the road marking samples. Dashed white markings were always on the left side of the lanes while solid ones were on the right side. Each label in Table 1 had a matching number that indicated its location. For instance, the road markings D1 and S1 were on the opposite sides of the same lane. Yellow markings W1 and W3 correspond for left and right side of the first work zone while W2 and W4 are located on a second work zone.

2.2. Photometric properties

The photometric properties, meaning luminance coefficients R_L and Q_d , were measured according to standard EN 1436 and averaged for every section. R_L was measured with static and dynamic measurement systems according to Babić et al. (2017). While the dynamic measurements provided a continuous result of how the road marking reflects the light from the head beam at exactly 30-m distance, static measurements operate on a spot-check basis. Q_d was measured only with static systems, since dynamic measurement systems cannot measure Q_d . To calculate the contrast between road markings and adjacent road surface additional static Q_d and R_L measurements were conducted on the road surface. Q_d could not be measured in the work zones, because they were not accessible on foot. It was observed that Q_d values of the pavement changed a lot, while R_L values changed only slightly. To compare photometric parameters with MD parameters that considered image contrast, Q_d -contrast between the Q_d value of the marking (I_m) and the Q_d value of the pavement (I_p) was calculated. Weber contrast was used, which is a common way to measure luminance differences.

$$\text{Weber contrast} = \frac{I_m - I_p}{I_p} \quad (1)$$

2.3. Weather data and light conditions

The visibility and detectability of road markings may depend on external factors such as weather, time of day, and surface wetness. To examine these factors, four surveys on each section under different conditions were conducted, which were labelled by daytime and surface wetness in Table 2. The sections were close to each other, so that the conditions studied were not only consistent within the sections, but also across all of the sections.

At night, the road was neither illuminated by streetlights nor by other notable light sources such as nearby buildings. However, apart from the test vehicle's own lighting and its reflections, the street was lit by nearby cars. To ensure comparable measurements, the speed has been adjusted when approaching a road segment to ensure no other cars were nearby. Backlight was minimized due to the distance between the rightmost lane and the lanes in the opposite direction, as well as the physical barrier separating them.

Rainfall intensities were extracted from the RADOLAN dataset, provided by the German meteorological service (DWD). The RADOLAN dataset offers 5-min radar precipitation data, calibrated with meteorological station measurements, at a spatial resolution of $1 \text{ km} \times 1 \text{ km}$. These data were matched to the 100 m segments and specific time of the survey. The survey under night/wet condition took place during a 30 min rain event with an extrapolated precipitation intensity of 1 mm/h, which can be described as heavy drizzle or light rain. The surface however was wet already due to a 15 min rain event (2 mm/h). It was assumed that all sections had adequate drainage properties, so they were equally wet.

2.4. Vehicle used to inspect the sections

The test vehicle used was developed for level 1–5 automation functions (Fig. 2). It was equipped with an InCar-PC, a NVIDIA Drive PX2, a dSPACE Microautobox II, and an Oxts RT3000 RTK-GNSS system for localisation. The camera system was attached to a camera bracket installed behind the windshield. The bracket ensures that a common angle and position of the camera system is applied. The LiDAR system was installed on the roof rack of the car that secured the sensor in place. Camera and LiDAR system were connected to the PC-systems via an Ethernet cable for data transfer and control. During the test drives the data was stored locally. Later the data spatially related to the section was extracted.

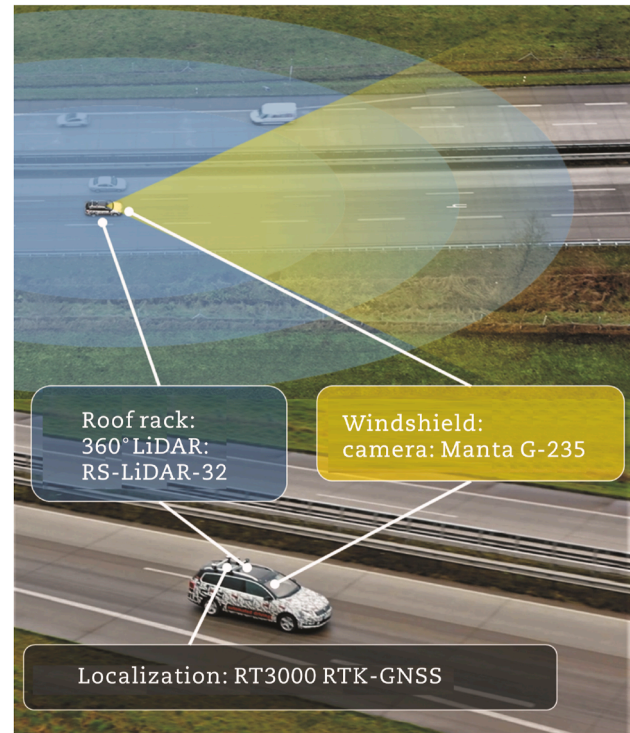


Fig. 2 – Test vehicle and equipment used in the surveys.

2.5. Technical characteristics of the camera system

An Allied Vision Manta G-235 camera system was used to collect image data. This camera has a compact and light-weight body with a 2.4 megapixel CMOS sensor. It can capture high-resolution images and videos in various lighting conditions with a dynamic range of 15 stops and a range of 100–51,200, as defined by ISO 12232. The system also supports 4 K video recording at up to 30 fps with HDR and Dolby vision. The Manta G-235 has a compact lens with a focal length of 12 mm and an aperture range of F1.4–16. The image sensor format equals $1/1.2''$ and the sensor provides a pixel size of $5.86 \mu\text{m} \times 5.86 \mu\text{m}$, resulting in an image resolution of $1936\text{H} \times 1216\text{V}$ (2.4 megapixels). The lens has a field of view of approximately 48° , which covers the area of interest for the experiments.

2.6. Technical characteristics of the LiDAR system

The LiDAR system used was the Robosense RS-LiDAR-32, which is a 360° surround-view sensor that uses a laser with a wavelength of 905 nm and a maximum range of 200 m. It has an optical aperture angle of 360° horizontally and 40° vertically. The system is equipped with 32 layers, allowing for detailed data capture of the surrounding environment. The system has a high accuracy of $\pm 3 \text{ cm}$. The LiDAR system was chosen because it offers a high-performance and reliable solution for autonomous driving applications, as it can provide a comprehensive and accurate 3D representation of the road scene with a high update rate of 20 Hz.

Table 2 – Characteristics of the four data collection runs.

Survey	Weather condition	Temperature/humidity
Day/moist	Overcast	15 °C/88%
Day/dry	Overcast	15 °C/82%
Night/dry	Clear	12 °C/82%
Night/wet	Rain	12 °C/94%

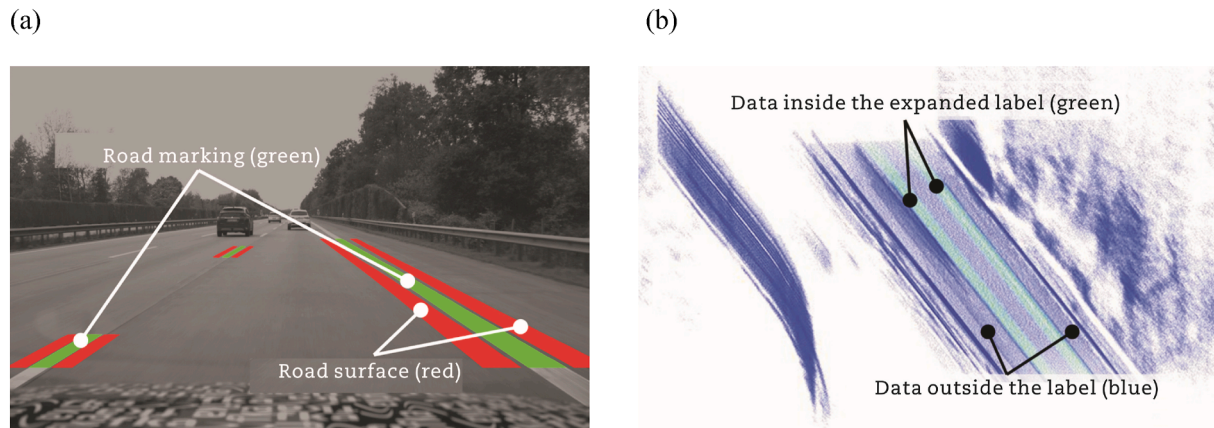


Fig. 3 – Camera image and LiDAR point cloud labelling. (a) Labels for contrast detection in the camera image. (b) LiDAR point cloud with highlighted data inside the expanded label.

2.7. Road marking labelling of the images in camera images

Pictures of the road were taken every 10 m, resulting in 10 pictures per 100 m section. The pixels that belonged to the road markings were manually segmented and manually labelled, as shown by the green area in Fig. 3(a). The road markings in 10–30 m distance from the camera were analysed. It was made sure that no cars obstructed the view. A 5 m wide evaluation area on the road was also selected, with a margin of road surface (equal to the width of a road marking) on both sides of each image. For work zones, the evaluation area was reduced to 4 m due to the narrower lanes.

2.8. Road marking labelling of the LiDAR point clouds

The LiDAR system produced a point cloud comprised of distinct data points. Each of these points was distinguished by its return intensity and three spatial dimensions, all relative to the location of the test vehicle, as shown in Fig. 3(b). The analysis focused on data points collected in the direction of travel between the locations where the initial and final images were obtained.

Labels manually embedded in the images facilitated the analysis of the LiDAR data. Given the established relative orientation among the camera, LiDAR, and road surface, these labels were modified for usage in marking the LiDAR data points. Any minor inconsistencies caused by irregularities in the road surface were addressed by implementing a refined labelling technique for the LiDAR data. This technique involved strategically expanding the dimensions of the labels to exactly twice their original width. One can think of these labels as bounding boxes utilized to classify the LiDAR points, as depicted by the green areas in Fig. 3(b). This expansion guaranteed the thorough capture of data points representing road markings.

In addition, the intensity value of each LiDAR data point could be understood as its reflectance attribute. Because the labels are exactly double the width of the road marking and the density of the data points remain constant, the median intensity value within the expanded labels functioned as a threshold to distinguish between data points corresponding to road markings and those indicating the road surface.

2.9. Preprocessing

The pictures with white road markings were converted to greyscale. However, for yellow markings in work zones the colour is relevant. Thus, a special setting was applied, using the positive range of the b-channel of the lab-colour space. Additionally, a normalization process is applied to the night-time images, taking into account the horizontally varying lighting intensity of the head lights, and facilitating a comparative analysis of the markings on the left and right side. Moreover, a Gaussian filter with $\sigma = 3$ was used to smooth the pictures and enhance the edges (Amaradi et al., 2016).

2.10. Machine detectability of road markings: contrast analysis

To investigate whether a correlation exists between machine detectability (MD) parameters and common photometric road markings parameters, MD needs to be derived from labelled sensor data. A straightforward approach is to analyse contrast, using two parameters: $MD_{\text{Contrast, Cam}}$, produced using camera images, and $MD_{\text{Contrast, LiDAR}}$, produced using LiDAR images. In image and point cloud processing, contrast is essential for segmentation, especially when thresholding techniques like Otsu's method (Otsu, 1979) are applied. Higher contrast leads to a larger range of possible thresholds, generally making threshold selection more robust (Kim et al., 2019). The contrast parameters are computed by calculating the mean values of pixel or data point intensities of the markings, using the same Weber contrast definition (1) as for the photometric properties. The affiliation of the pixels and data points is determined by the labels described earlier.

2.11. Machine detectability of road markings: gradient and edge analysis

To further explore whether solely analysing image contrast is adequate for describing machine detectability (MD), two new parameters, MD_{Gradient} and MD_{Edge} , have been introduced. These are derived from image processing metrics like Sobel

and Canny algorithm. Table 3 gives an overview over the MD parameters defined in this work. In the following, Table 4 is used to illustrate the image processing metric behind MD_{Gradient} and MD_{Edge} for three sample images.

MD_{Gradient} is calculated by applying a Sobel filter (Kanopoulos et al., 1988) to the blurred images, as shown in Table 4, row 2 (gradient image). In image processing, intensity gradients between pixels serve as input for robust and binarising edge detection methods, such as the Canny algorithm (Canny, 1986). High gradients are crucial for creating binary edge images (Amaradi et al., 2016). MD_{Gradient} quantifies the quality of the marking with respect to edge feature extraction. It is defined as the mean of gradient values along the marking edges, where the marking edges are identified as the maximum gradient pixel in the horizontal direction, as suggested in the studies of Lim and Braunl (2019), Veit et al. (2008), and Haloi and Jayagopi (2015).

MD_{Edge} quantifies the suitability of marking edges for extraction of ridges as a feature. Popular ridge detection algorithms are Hough transform (Duda and Hart, 1972), RANSAC (Fischler and Bolles, 1981), and polynomial fitting. To fit the marking to a ridge model, Bezier curves (Huang et al., 2013) and straight lines (Amaradi et al., 2016) are commonly used. Here, high-intensity edges at the markings edge positively impact edge detection, while high-intensity edges associated with non-marking objects limit ridge detection applicability. MD_{Edge} reflects both effects.

The Canny operator is commonly used to generate input for ridge detection by thinning and binarising the edges of the gradient image (Canny, 1986). Canny algorithm is applied with minimum T_1 and $T_2 = 1/2^8$ (8 bit image) showing all potential Canny edge pixels, as presented in Table 4, row 3 (Canny image). The maximum gradient information is used to label the edge pixels.

To calculate MD_{Edge}, Canny algorithm is used in reverse.

- (1) The sensitivity was set at 80%, while the specificity was set at 99%. These levels of sensitivity and specificity were chosen to represent about the same number of pixels: on average, the evaluated road surface had about 20 times more potential Canny edge pixels than the marking edges in the analysed data.
- (2) The thresholds (T_{SEN} , T_{SPE}) needed to realise the binary classifiers (setting $T_1 = T_2$ in both cases) were applied to the Canny image, as visualised in Table 4, row 4 (T_{SEN}) and row 5 (T_{SPE}).

- (3) By dividing the two thresholds, MD_{Edge} was estimated.

$$MD_{Edge} = \frac{T_{SEN80}}{T_{SPE99}} \quad (2)$$

In Eq. (2), MD_{Edge} > 1 means that a sensitivity of 80% and a specificity of 99% is possible. The higher MD_{Edge}, the wider is the span for possible thresholds that fulfil these conditions.

2.12. Regression analysis and quotient comparison

The MD results are determined for every image and then averaged for every section. To address research question A, if a correlation between MD and common photometric road marking parameters (R_L , Q_d) can be established, a linear regression was conducted between common photometric parameters and MD_{Contrast} parameters. Linear regression was found suitable because the photometric parameters (Q_d and R_L) have been designed to quantify visibility by human drivers under small inclination angles from a car seat perspective in specified lighting scenarios. Specifically, the MD_{Contrast,Cam} parameter derived from daytime images is correlated with Q_d -contrast. Additionally, the MD_{Contrast,Cam} parameter from nighttime images and MD_{Contrast, LiDAR} from all LiDAR-point clouds were correlated with R_L .

To assess the quality and reliability of the linear regression models in this study, several statistical diagnostics were conducted.

- (1) Normality of residuals (NoR) is examined using Anderson-Darling test, where a low p -value <0.05 indicates a departure from normality. If the distribution of the residuals is departing from normality the linear regression is not valid. A p -value >0.05 is not challenging the validity of the model.
- (2) Significance of slope: if the p -value associated with the slope coefficient (m) is < 0.05, it indicates a statistically significant difference from a model with a constant, zero slope, suggesting that the photometric road marking parameter (such as R_L and Q_d) has a significant effect on the MD parameter.
- (3) Positive slope requirement: m has to be greater than zero. This requirement, combined with a statistically significant p -value (<0.05), confirms a meaningful and

Table 3 – MD parameter overview.

Sensor	MD parameter	Description
Camera	MD _{Contrast,Cam}	Suitability of the marking for image segmentation methods (e.g., Otsu's method)
	MD _{Gradient}	Quality of the marking with respect to edges as a feature (e.g., Sobel algorithm)
	MD _{Edge}	Suitability of marking edges for extraction of ridges as a feature (e.g., Canny algorithm)
LiDAR	MD _{Contrast, LiDAR}	Suitability of the marking for point cloud segmentation methods (e.g., Otsu's method)

Table 4 – Image processing metric applied to a specific road scene in three different conditions.




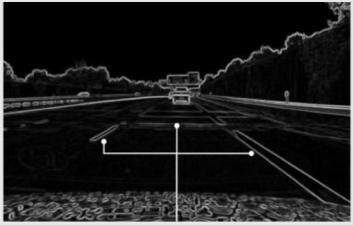

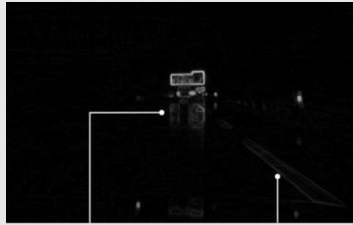
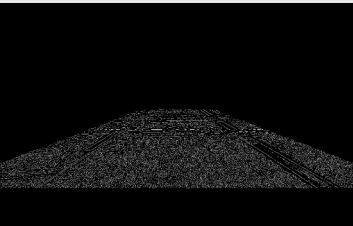
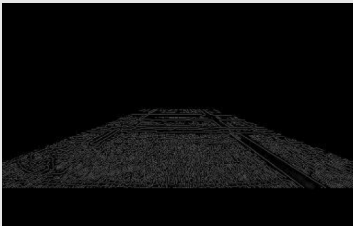
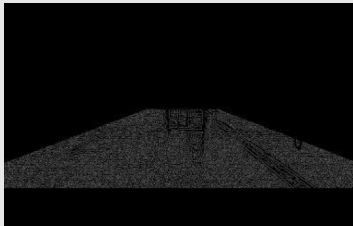
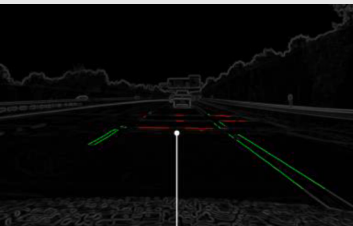
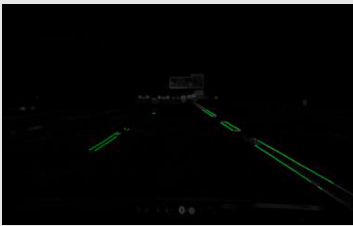
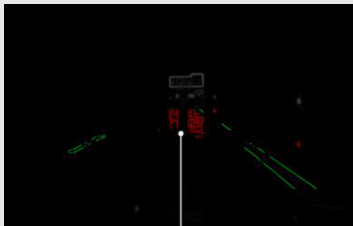
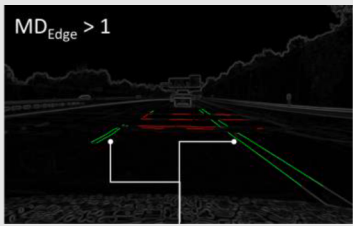
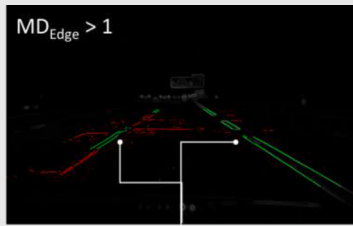

	Day/dry	Night/dry	Night/wet
Original image			
Gradient image MD _{Gradient}			
	Medium gradients on marking edges and asphalt patch	Low gradients and high gradients on marking edges	Medium gradients low gradients on reflections on marking edges
Canny image ($T = 0$)			
Canny image (T_{SEN80}) MD _{Edge}			
	False positive edges (red) on asphalt patch	No false positive edges	False positive edges (red) on reflection
Canny image (T_{SPE99}) MD _{Edge}			
	True positive edges (green) cover all road marking edges	True positive edges (green) cover all road marking edges	True positive edges (green) rarely cover road marking edges

Table 5 – R_L and MD parameters for the markings evaluated (nighttime).

Marking type	Marking	$R_L \downarrow$	Night/dry				Night/wet			
			MD _{Contrast,Cam}	MD _{Gradient}	MD _{Edge}	MD _{Contrast, LiDAR}	MD _{Contrast,Cam}	MD _{Gradient}	MD _{Edge}	MD _{Contrast, LiDAR}
Dashed and solid white flat marking	S2	531	8.310	0.1120	38.950	6.650	2.770	0.0080	2.670	0.910
	S3	374	8.580	0.1060	26.250	5.920	0.940	0.0080	0.480	0.570
	D1	296	5.280	0.0770	33.510	4.710	1.580	0.0060	2.060	0.400
	S1	111	3.760	0.0490	18.220	1.520	0.690	0.0030	0.950	0.780
	D3	40	1.990	0.0400	8.540	0.140	0.350	0.0020	0.040	0.340
	D2	38	1.980	0.0310	9.370	0.180	0.630	0.0030	0.700	1.010
	Mean	232	4.980	0.0690	22.470	3.190	1.160	0.0050	1.150	0.670
	p-value NoR NoR	(>0.05)	0.200	0.5400	0.410	0.700	0.210	0.4000	0.210	0.600
	p-value m	(<0.05)	0.000	0.0000	0.010	0.000	0.020	0.0100	0.100	0.860
	m	(>0)	0.014	0.0002	0.059	0.014	0.004	0.0000	0.004	0.000
	p-value b	(>0.05)	0.060	0.0000	0.050	0.800	0.450	0.0400	0.580	0.030
	b	(\approx 0)	1.750	0.0300	8.880	-0.120	0.260	0.0020	0.300	0.640
	R ²		0.910	0.9600	0.880	0.960	0.780	0.8800	0.540	0.010
Dashed and solid white structured marking	S5	265	5.900	0.0880	30.380	3.540	6.800	0.0220	8.450	0.850
	D5	245	5.820	0.1190	41.070	2.170	6.130	0.0260	10.070	0.470
	S4	227	5.970	0.0710	29.380	2.530	6.440	0.0230	8.340	1.100
	D4	213	5.720	0.0660	24.670	1.730	3.380	0.0130	4.770	0.420
	D7	113	5.290	0.0630	23.040	1.680	1.830	0.0060	1.990	0.880
	S7	107	4.850	0.0560	22.470	2.220	4.160	0.0110	3.570	1.030
	D6	67	2.910	0.0420	11.850	0.550	1.180	0.0050	1.420	0.820
	S6	59	2.520	0.0320	8.830	1.600	1.900	0.0050	1.650	0.780
	Mean	162	4.870	0.0670	23.960	2.000	3.980	0.0140	5.030	0.790
	p-value NoR	(>0.05)	0.800	0.4500	0.140	0.570	0.840	0.9700	0.830	0.990
	p-value m	(<0.05)	0.000	0.0100	0.000	0.030	0.000	0.0000	0.000	0.520
	m	(>0)	0.014	0.0003	0.107	0.008	0.024	0.0001	0.038	-0.001
	p-value b	(>0.05)	0.010	0.1200	0.180	0.180	0.890	0.6400	0.330	0.000
	b	(\approx 0)	2.550	0.0230	6.560	0.770	0.130	-0.0010	-1.180	0.920
Workzone yellow marking	R ²		0.760	0.7100	0.770	0.550	0.780	0.8400	0.860	0.070
	W1	62	7.300	0.0080	1.140	—	1.980	0.0100	0.640	—
	W2	36	14.630	0.0050	0.550	—	2.410	0.0030	0.070	—
	W3	35	7.400	0.0070	1.730	—	1.740	0.0020	0.040	—
	W4	35	9.230	0.0070	1.480	—	4.140	0.0020	0.080	—
	Mean	42	9.640	0.0070	1.230	—	2.570	0.0040	0.210	—
	p-value NoR	(>0.05)	0.540	0.1400	0.480	—	0.700	0.1400	0.610	—
	p-value m	(<0.05)	0.580	0.3600	0.850	—	0.630	0.0000	0.000	—
	m	(>0)	-0.109	0.0001	-0.006	—	-0.030	0.0003	0.022	—
	p-value b	(>0.05)	0.190	0.2000	0.340	—	0.240	0.0100	0.000	—
	b	(\approx 0)	14.220	0.0040	1.460	—	3.830	-0.0080	-0.700	—
	R ²		0.180	0.4000	0.020	—	0.140	0.9900	1.000	—

Note: several regression analyses were conducted for each marking type and every MD parameter, under both night/dry and night/wet conditions; \downarrow indicates that the data is sorted by R_L ; however, not all regression results are valid because some did not meet the requirements of the preceding results (given in brackets); bold entries signify valid results that are analysed and discussed.

Table 6 – Q_d -contrast (camera)/ R_L (LiDAR) and MD parameters for the markings evaluated.

Marking type	Marking	Q_d -contrast ↓	Day/dry				Day/moist			
			MD _{Contrast,Cam}	MD _{Gradient}	MD _{Edge}	MD _{Contrast, LiDAR}	MD _{Contrast,Cam}	MD _{Gradient}	MD _{Edge}	MD _{Contrast, LiDAR}
Dashed and solid white flat marking	D1	2.75	0.550	0.0490	6.070	5.080	0.550	0.0490	6.070	5.080
	D2	2.35	0.540	0.0460	5.910	0.180	0.540	0.0450	5.210	0.190
	D3	2.22	0.600	0.0490	4.930	0.140	0.570	0.0470	5.390	0.170
	S3	1.25	0.740	0.0550	5.390	6.350	0.730	0.0560	6.130	6.210
	S2	1.21	0.810	0.0590	7.010	6.690	0.780	0.0580	6.640	6.680
	S1	0.86	0.760	0.0570	6.860	1.560	0.760	0.0570	6.860	1.560
	Mean	1.77	0.670	0.0530	6.030	3.330	0.650	0.0520	6.050	3.310
	p-value NoR	(>0.05)	0.570	0.2200	0.120	0.600	0.470	0.8900	0.450	0.440
	p-value m	(<0.05)	0.000	0.0200	0.330	0.000	0.000	0.0200	0.090	0.000
	m	(>0)	−0.145	−0.0058	−0.512	0.015	−0.142	−0.0063	−0.642	0.015
	p-value b	(>0.05)	0.000	0.0000	0.000	0.900	0.000	0.0000	0.000	0.920
	b	(≈0)	0.920	0.0630	6.940	−0.070	0.910	0.0630	7.190	−0.060
	R ²		0.900	0.7900	0.230	0.940	0.920	0.7600	0.560	0.940
Dashed and solid white structured marking	D4	2.00	0.620	0.0530	6.960	1.800	0.620	0.0530	6.700	1.810
	D5	2.00	0.510	0.0490	7.040	2.120	0.570	0.0510	7.500	2.320
	D7	1.97	0.630	0.0550	9.430	1.960	0.580	0.0520	7.770	2.070
	D6	1.82	0.620	0.0540	7.860	0.670	0.570	0.0520	6.630	0.890
	S5	1.16	0.670	0.0520	7.290	3.740	0.670	0.0510	7.390	3.830
	S7	1.14	0.730	0.0570	9.180	2.290	0.710	0.0560	7.750	2.370
	S6	0.97	0.640	0.0530	7.300	1.610	0.630	0.0520	6.360	1.730
	S4	0.80	0.610	0.0480	6.010	2.530	0.590	0.0470	5.640	2.620
	Mean	1.48	0.630	0.0530	7.630	2.090	0.620	0.0520	6.970	2.210
	p-value NoR	(>0.05)	0.580	0.5600	0.190	0.490	0.620	0.4300	0.710	0.810
	p-value m	(<0.05)	0.220	0.6800	0.500	0.050	0.190	0.4400	0.260	0.050
	m	(>0)	−0.059	0.0009	0.630	0.007	−0.051	0.0015	0.668	0.007
	p-value b	(>0.05)	0.000	0.0000	0.000	0.140	0.000	0.0000	0.000	0.090
	b	(≈0)	0.720	0.0510	6.700	0.890	0.690	0.0500	5.980	1.040
	R ²		0.240	0.0300	0.080	0.510	0.260	0.1000	0.200	0.510
Workzone yellow marking	W1	—	33.170	0.0330	8.570	—	25.830	0.0340	8.780	—
	W2	—	6.460	0.0290	6.550	—	8.130	0.0300	6.650	—
	W3	—	4.060	0.0280	4.240	—	4.060	0.0280	4.240	—
	W4	—	22.830	0.0260	4.820	—	22.830	0.0260	4.820	—
	Mean	—	16.630	0.0290	6.050	—	15.210	0.0290	6.120	—

Note: several regression analyses were conducted for each marking type and every MD parameter, under both day/dry and day/moist condition; ↓ indicates that the data is sorted by Q_d -contrast; however, not all regression results are valid because some did not meet the requirements of the preceding results (given in brackets); bold entries signify valid results that are analysed and discussed.

Table 7 – Established correlations between MD parameters and common photometric road marking parameters.

Sensor	MD parameter	Environmental condition and marking type											
		White flat marking				White structured marking				Yellow marking			
		Night/ dry	Night/ wet	Day/ dry	Day/ moist	Night/ dry	Night/ wet	Day/ dry	Day/ moist	Night/ dry	Night/ wet	Day/ dry	Day/ moist
Camera	MD _{Contrast,Cam}	✓	✓	×	×	✓	✓	×	×	×	×	–	–
	MD _{Gradient}	✓	✓	×	×	✓	✓	×	×	×	×	–	–
	MD _{Edge}	✓	×	×	×	✓	✓	×	×	×	×	–	–
LiDAR	MD _{Contrast, LiDAR}	✓	×	✓	✓	✓	×	✓	✓	–	–	–	–

Note: ✓ indicates research question A is verified, × indicates research question A is not verified, – indicates the condition was not analysed.

positive relationship between the MD parameters and standard photometric parameters.

- (4) Analysis of intercept (*b*): an intercept approximately equal to 0 or with a *p*-value >0.05 suggests that the intercept does not significantly differ from zero, which is essential to ensure that the model does not have a bias due to a non-zero intercept.
- (5) Model fit (R^2): after the above criteria are met, the overall fit of the model to the data is evaluated using the coefficient of determination (R^2). A higher R^2 value indicates a better fit of the model to the observed data.

For research question B, which investigates whether a multi-MD-parameter approach can reveal effects on the MD of road markings, which are not captured by image contrast analysis alone, quotients (MD_1/MD_2) are calculated. These demonstrate the relationship between specific MD_1 and MD_2 parameters under varying environmental conditions. Practically, $MD_{Contrast,Cam}/MD_{Gradient}$ and $MD_{Gradient}/MD_{Edge}$ will be compared under night/dry, night/wet and day/dry conditions to draw further insights.

The quotients are analysed as followed: If the parameters MD_1 and MD_2 perform the same way in different conditions, the quotient MD_1/MD_2 would be the same in all conditions. In that case, one parameter would be enough to describe machine detectability (MD). But if MD_1/MD_2 are varying when looking at different condition one parameter is not enough and research question B is answered negatively.

3. Results

3.1. Qualitative results

Before comparing the MD parameters to conventionally measured parameters and among each other on a quantitative basis, the process of MD analysis is imaged qualitatively in Table 4. All pictures in Table 4 show the very same scene and the exact same road markings under varying conditions. Because of the transparent and differentiated approach defined in the previous chapter different qualitative phenomena can be spotted during the analysis of contrast, gradients, and edges. The approach evaluates the input quality for common feature extraction methods listed in Table 3.

The following effects are highlighted in Table 4: high and low gradients are highlighted with different levels of

brightness in row 2 (gradient images). In row 3 Canny algorithm with a threshold of 0 is applied to the gradient images, showing all potential edges that Canny algorithm can detect. Row 3 and 4 show only a part of these potential edges, depending on the threshold applied (row 3: T_{SEN80} , row 4: T_{SPE99}). In row 4, the gradient-threshold T_{SEN80} , which realises a sensitivity of 80%, is applied to the full Canny image (row 3), leaving potential false-positive edges displayed in red. In row 5, on the other hand, the gradient-threshold T_{SPE99} , which realises a specificity of 99% is applied, showing only marking edges (labelled green) that raise above the threshold T_{SPE99} and show a good potential for true-positive detection labelled green.

This paper aims to address the gap in road marking detectability and propose a transparent signal processing metric to determine MD of road markings. This metric includes a new set of MD parameters that evaluate the input quality for common feature extraction methods, such as thresholding, edge detection, and ridge detection.

In Table 4, specifically in row 4 (T_{SEN80}), the presence of red edges highlights the issue of potential false-positive detections: If an intensity threshold is determined to detect 80% of the marking edges (T_{SEN80}), non-marking edges exist, which have a risk of being false-positive detected. For instance, asphalt patches (column 1) or reflections on wet surface (column 3) could significantly interfere with the accurate detection of road markings, primarily due to the increased likelihood of false-positive detections.

Furthermore, it is worth noting that the asphalt patch is not visible during nighttime, whether the road is dry (column 2) or wet (column 3). Similarly, there are no reflections from the traffic sign under dry conditions, during either daytime (column 1) or nighttime (column 2). Without even analysing MD parameters, this already indicates that it is not possible to infer results from one condition to another, even when the very same section is assessed.

3.2. Quantitative results

Tables 5 and 6 show the MD results of the sections. The MD results are listed alongside the corresponding common photometric road marking parameters (R_L - and Q_d -contrast). To facilitate a quick analysis of a linear correlation, the table entries are arranged in ascending order based on R_L - and Q_d -contrast, as indicated by the arrow in each table header. The expectation was that as R_L - and Q_d -contrast values decrease, the MD values would proportionally decrease.

Moreover, road markings were categorised into three distinct types: flat, structured, and yellow. For each type, a detailed linear regression analysis was conducted to evaluate their performance characteristics under various conditions. The analysis focused on five key aspects to assess the robustness and relevance of the regression models. If an aspect was not fulfilled, the remaining aspects are not analysed anymore because in such cases the research question was already answered negatively. Only the aspects that were analysed are shown in bold in [Tables 5 and 6](#)

Firstly, it was validated that the residuals derived from the regression models follow a normal distribution, which confirms the applicability of linear regression to the datasets. It was concluded that all categories of road markings met this fundamental criterion (p -value > 0.05), thereby affirming the appropriateness of employing linear regression in the study.

Secondly, the analysis compared the linear model to a simple constant model ($m = 0$). To prove a significant influence of common photometric parameters (R_L and Q_d) on MD, the linear model needs to supersede the constant benchmark significantly. In several cases, the linear model did not significantly outperform the constant model. (1) $MD_{\text{Contrast, LiDAR}}$ under night/wet conditions. (2) MD_{Edge} for flat markings under night/wet conditions. (3) MD_{Edge} under daytime conditions. (4) MD_{Contrast} and MD_{Gradient} for structured markings under daytime conditions. (5) MD_{Contrast} and MD_{Gradient} in most cases with yellow markings. This suggested that, in these specific cases, the common photometric parameters might not be the primary influencers on MD. This result could imply that other, unmeasured variables might be playing a more significant role, or that the relationship between was not linear, as hypothesised. Such cases should be the subject of future investigations.

Thirdly, m in those linear models that significantly outperform a constant model was analysed. Most of the cases demonstrated a positive slope. This was the expected because a positive slope indicates that MD improves along with the common photometric parameters (R_L and Q_d). However, some cases were expectation: MD_{Contrast} and MD_{Gradient} for flat markings in daytime conditions. A negative slope implies that the impact is marginal and that unmeasured variables have a stronger impact on MD than the common photometric parameters.

Fourthly, b of the linear models was studied. Ideally, for a valid model, the intercept should be near zero or not significantly different from zero. This occurs when p -value $b > 0.05$ or when $b \approx 0$. While this was true in most cases, exceptions were noted in cases involving yellow road markings in both and dry conditions, particularly for the models concerning MD_{Gradient} and MD_{Edge} . This could indicate a baseline level of visibility or effectiveness that is inherently different for yellow markings compared to others.

Lastly, the effectiveness of the linear models was evaluated using the coefficient of determination R^2 . Among the remaining cases, where the linear models have a positive slope, intercept the vertical axis near 0 and differ significantly from a constant model, R^2 was always > 0.50 : (1) $MD_{\text{Contrast, Cam}}$ for white markings in nighttime conditions (R^2 from 0.76 to 0.91), (2) MD_{Gradient} for white markings in nighttime conditions (R^2 from 0.71 to 0.96), (3) MD_{Edge} for white, structured markings in nighttime conditions (R^2 from 0.77 to 0.86), (4) MD_{Edge} for white, flat markings in night/dry conditions ($R^2 = 0.88$), (5) $MD_{\text{Contrast, LiDAR}}$

for white, flat markings in dry or moist conditions (R^2 from 0.94 to 0.96), and (6) $MD_{\text{Contrast, LiDAR}}$ for white, structured markings in dry or moist conditions (R^2 from 0.51 to 0.55).

4. Discussions

4.1. Research question A

As mentioned above, research question A explores whether there is a correlation between MD parameters and common photometric road marking parameters, namely retroreflectivity (R_L) and daytime visibility (Q_d). The previous section presented the outcomes of testing the efficiency and consistency of a linear regression model linking the MD parameters with these photometric road marking parameters. [Table 7](#) summarises the conditions under which a correlation between MD parameters and standard photometric road marking parameters can be established.

Under certain conditions, a correlation was found between MD parameters and the standard photometric road marking parameters in the data collected in this study. Research question A was verified in various cases. In nighttime conditions, R_L , the determinant for retroreflectivity, was found to be a consistent predictor for both contrast and edge intensity of white road markings captured in camera images, regardless of the road's condition being dry, moist, or wet. The results regarding the contrast-based parameters align with findings from closed track tests. In [Burghardt et al. \(2023\)](#) and [Pike et al. \(2019\)](#), R_L also proved to be a consistent predictor for image contrast. Additionally, R_L was effective in predicting contrast in the studied LiDAR point clouds under dry or moist conditions, applicable during both day and night.

This confirms the results found in [Burghardt et al. \(2021b\)](#), which also noted that LiDAR systems struggle to distinguish wet road markings from the road surface. This consistent finding underscores the need for further improvements in LiDAR technology or complementary methods to enhance detectability under wet conditions.

However, there were limitations to the correlation asked for in research question A. Under wet conditions, R_L proved to be an inconsistent predictor for contrast in LiDAR point clouds, as evidenced by the linear model's lack of significant deviation from a constant model. This indicates that the LiDAR technology used is more negatively influenced by wetness than the camera employed in the investigation. This conclusion concurs with [Burghardt et al. \(2021b\)](#), where LiDAR also showed weaknesses at distinguishing wet road markings from road surface. One should observe here that R_L measured under the conditions of wetness (usually referred to as RW) could provide more valid parameter; it was not assessed within the scope of this study.

It is important to note that these results are based on tests conducted on straight road segments. The results may not be applicable to curved roads, where altering viewing angles can significantly affect detectability. Furthermore, the study did not account for adverse weather conditions beyond light rain, such as heavy rain or snow, nor did it consider adverse lighting conditions like glare from other vehicles, low sun, or streetlights.

Table 8 – Ranked MD parameter performance in different environmental conditions.

Sensor	MD parameter	Environmental condition and marking type											
		White flat marking				White structured marking				Yellow marking			
		Night/ dry	Night/ wet	Day/ dry	Day/ moist	Night/ dry	Night/ wet	Day/ dry	Day/ moist	Night/ dry	Night/ wet	Day/ dry	Day/ moist
Camera	MD _{Contrast, Cam}	▼▼	▼▼	▼▼	▼▼	★★	★★	★★	★★	▲▲	▲	▲▲	▲▲
		▼▼	▼			★★	★					▲▲	▲▲
	MD _{Gradient}	★★	★	★★	★★	▲▲	▲	▲▲	▲▲	●●	●	●●	●●
		★★		★	★	▲▲		▲	▲			●●	●●
LiDAR	MD _{Edge}	▲▲	▲	▲▲	▲▲	●●	●	●●	●●	▼▼	▼	▼▼	▼▼
		▲▲		▲	▲	●●		●				▼▼	▼▼
	MD _{Contrast, LiDAR}	●●	●	●●	●●	▼▼	▼	▼▼	▼▼	–	–	–	–
		●●		●●	●●	▼▼		▼▼	▼▼				

Note: conditions are ranked within every MD parameter for each marking type; four identical symbols denote the best-performing condition, one symbol denotes the worst-performing condition, and a dash (–) shows that the condition was not analysed; to prevent confusion between marking types, the symbol assignment changes with the marking type; for the white flat marking, ▼ = MD_{Contrast, Cam}, ★ = MD_{Gradient}, ▲ = MD_{Edge}, ● = MD_{Contrast, LiDAR}; for the white structured marking, ★ = MD_{Contrast, Cam}, ▲ = MD_{Gradient}, ● = MD_{Edge}, ▼ = MD_{Contrast, LiDAR}; for the yellow marking, ▲ = MD_{Contrast, Cam}, ● = MD_{Gradient}, ▼ = MD_{Edge}, as the LiDAR parameter was not analysed, no symbol is shown; symbol counts show relative performance only within the same MD-parameter and marking type group; do not compare counts across different rows or columns.

Additionally, it was noted that Q_d -contrast, the contrast of the determinant for daylight visibility, is an unreliable predictor for camera contrast or other camera-based MD parameters. This is unexpected considering that Q_d is also measured with the 30 m-geometry and uses the same principle and unit of a luminance coefficient. A likely explanation for Q_d -contrast being an unreliable predictor is that the maximum pixel intensity of the imaged road markings was reached across the entire dataset, which agrees with the outcome from unrelated research (Burghardt et al., 2023). This implies that beyond a certain threshold of the camera settings, increasing Q_d does not enhance contrast in a daytime camera image. It is plausible that this threshold of saturation has been surpassed within the dataset of this study. Considering that the lowest Q_d value in the dataset was 124 mcd/lx/m², which is well above the recommended threshold value for renewal according to German guidelines (104 mcd/lx/m²), it is suggested to repeatedly apply the method for road markings with lower Q_d values, which are closer to the renewal threshold, in future research.

Yellow markings were exclusively analysed in nighttime conditions due to the absence of Q_d data. However, under the environmental conditions analysed and based on the dataset used, no correlations could have been established for any of the MD parameters applied. One potential explanation for this outcome is that the MD parameters were assessed based on the positive range within the b-channel of the lab-colour space. This implies that the retroreflectivity of yellow road markings may not necessarily correlate to their colour intensity, which agrees with the findings in Burghardt et al. (2019).

4.2. Research question B

4.2.1. Understanding road marking detectability through MD_{Gradient} and MD_{Edge} analysis

Research question B focused on the necessity of a multi-parameter approach, featuring MD_{Gradient} and MD_{Edge}, to address the limitations of relying solely on image contrast analysis and off-the-shelf machine vision systems for detecting road markings. While off-the-shelf systems offer realistic

analyses (Marr et al., 2020; Pappalardo et al., 2021; Pike et al., 2018a, 2018b), their complex image processing and ambiguous feature utilization make results hard to interpret, as highlighted in Marr et al. (2020). Image contrast analysis (Burghardt et al., 2021b, 2023), despite its transparency, lacks procedural depth by analysing only contrast as a feature.

MD_{Gradient} and MD_{Edge} were introduced to bridge this knowledge gap. MD_{Gradient} uses a unique image processing method to assess road marking visibility against the surrounding surface, similar to MD_{Contrast, Cam} but with a different approach. Additionally, MD_{Edge} extends the assessment beyond just the marking's edge intensity to include comparisons with non-marking elements on the road to encompass the entire road surface, providing a comprehensive view of marking detectability. This multi-parameter approach aimed to complement MD_{Contrast, Cam} and uncover aspects of MD of road markings not captured by sole contrast analysis or the use of off-the-shelf machine vision systems.

It can be observed that the correlation between MD_{Edge} and R_L in night and dry conditions was similar to that of MD_{Gradient} with R_L . This pattern also held for night and wet conditions when looking at structured road markings. However, for flat markings in wet conditions, R_L was not a reliable indicator for MD_{Edge}, though it continued to accurately predict MD_{Gradient} outcomes; as mentioned earlier, correlation with R_L measured in wet conditions could be more accurate. This is supported by data in Table 4, which shows that specular reflections, like those from traffic signs, mainly occur in night and wet conditions, as seen in row 3 of Table 4. In contrast, during night and dry conditions, see row 2 of Table 4, there is a minimal presence of specular reflection sources, as it has been described in reference (Saint-Jacques and Brémond, 2023). Road markings at night stand out from their surroundings due to its retroreflection properties, a fact noted in Burghardt et al. (2020). Yet, as Table 4 and Burghardt et al. (2023) showed, cameras face challenges distinguishing between specular and retroreflective reflections. This difficulty in differentiating reflections in wet conditions highlights the need for a parameter like MD_{Edge}, which

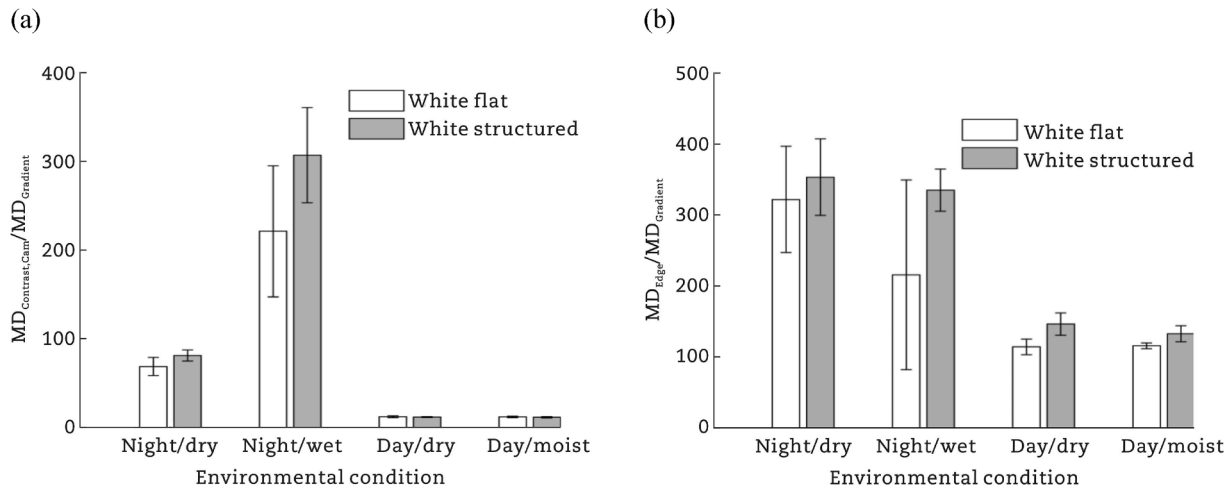


Fig. 4 – Comparative quotients of MD parameters for flat and structured white marking. (a) Ratio of $MD_{Contrast,Cam}$ to $MD_{Gradient}$. (b) Ratio of $MD_{Gradient}$ to MD_{Edge} .

quantifies the problems specular reflections add to the task of road marking detection.

4.2.2. Performance of MD parameters in different conditions

To consequently investigate into research question B, the performances of the MD parameters obtained under different environmental conditions were compared among each other in different environmental conditions. Given that research question B states that MD performance for road markings could not be fully captured by image contrast analysis alone, it was expected that the performance of the MD parameters would differ under various environmental conditions.

The performance of MD parameters is ranked in Table 8, which compares the mean values from Tables 5 and 6. For every combinations of MD parameter and marking type separate comparisons were conducted between the MD performances in different environmental conditions. The ranking was explicitly not applied between the MD parameters, nor between the marker types. The condition where the MD parameter performed best was given a 4-symbol rating, while the lowest received a 1-symbol rating. If two conditional mean values differed to a maximum of 5% from the common average, they were assigned the same rating to account for marginal differences. The validity of these rankings will be explored in the subsequent paragraphs.

The analysis of $MD_{Contrast,Cam}$ showed that white road markings, either structured and flat ones, were more visible against the road at night than during the day, regardless of the weather being rainy or dry. This outcome was expected for dry conditions, as R_L typically augments the contrast that is usually achieved with Q_d . This was expected because asphalt and concrete, which compromise road surfaces, are not designed to retroreflect light and appear black; in daylight conditions, road surfaces rather appear grey. To best of our knowledge, there are no standards that would define maximum or even any photometric properties of road surfaces. However, most international and national standards suggest similar minimum levels for R_L and Q_d . Furthermore, $MD_{Contrast,Cam}$

confirmed that road markings are more easily detected at night in dry conditions than in wet conditions or during daylight in dry conditions.

In terms of $MD_{Contrast,Cam}$, yellow markings outperform white ones, as observed in Tables 5 and 6, despite yellow markings having significantly lower R_L . The reason for this is that the yellow markings were assessed based on the positive range of the b-channel of the lab-colour space. In other words, the yellowness of the marking is compared to the yellowness of the road surface. Since road surfaces usually do not have colour components, coloured markings make a very good contrast, as already suggested in Storsæter et al. (2021b).

Yellow road markings show a distinct contrast advantage during the day, which diminishes at night, as indicated by their $MD_{Contrast,Cam}$ performance shown in Table 8. As highlighted in Storsæter et al. (2021b), the retroreflected light of many yellow marking products appears less yellow compared to their appearance under diffuse illumination. One possible explanation for this is that only the colour appearance under diffuse illumination is standardised by a standardised colorimetric locus. Following the principle of subtractive colour mixing, colouring a surface basically reduces its brightness compared to a white surface, which reflects all part of the light. Since there is no standard for colour appearance of retroreflected light, but requirements for total brightness (R_L) still apply, yellow markings are often only coloured yellow at the top surface of the plastic. They lack colour at the surface areas below the embedded glass beads, which are mainly responsible for retroreflection. Given that yellow markings strongly contribute to MD due to the enormous contrast in the lab-color space, standards lacking requirements of a colorimetric locus in retroreflective scenarios should be reconsidered. With nothing else on the road surface but road markings being coloured, resulting in very high contrasts, coloured markings become a viable alternative to white markings, especially for daytime detectability.

Thus far, $MD_{Contrast,Cam}$ has been discussed in detail. To address research question B, the findings regarding $MD_{Contrast,Cam}$

Cam are now opposed to those of MD_{Gradient} , MD_{Edge} , and $MD_{\text{Contrast, LiDAR}}$. The data indicates that daytime is the most challenging condition to detect white markings, as shown in Table 8, with night and wet conditions being less challenging, and night and dry conditions presenting the least difficulty. When examining Table 8 for MD_{Gradient} and MD_{Edge} , the order of performance changes compared to $MD_{\text{Contrast, Cam}}$. Daytime conditions generally allow for better camera detectability than night/wet conditions, but are surpassed by night/dry conditions. This shift in ranking can be explained by examining the results and images more closely. Notably, night/wet conditions fall behind day/dry conditions mainly because wetness tends to blur the edges of markings, making them appear less sharp in camera images.

Proceeding to the LiDAR sensor, $MD_{\text{Contrast, LiDAR}}$ shows consistent performance in both night/day and dry/wet conditions. It benefits from the retroreflective properties of road markings during the day as well as at night, leading to its performance being roughly three times higher than that of $MD_{\text{Contrast, Cam}}$ in daytime conditions, as shown in Tables 5 and 6. However, under wet conditions, the LiDAR performs at a similar level to the camera in daytime. Concurrently, the camera performs significantly better in night/wet conditions, three to five times higher than the LiDAR. This difference is significant even considering that $MD_{\text{Contrast, Cam}}$ is by far the best performing camera based parameter. LiDAR addresses the camera's limitations by enhancing marking detection during the day and complements the camera well in night/dry conditions. However, in wet conditions, the LiDAR might struggle to contribute to road marking detection, meaning that the focus in wet conditions is on camera detectability. Regarding research question B, a clear advantage of a multi-parameter or multi-sensor approach was demonstrated.

4.2.3. Quantitative analysis of MD parameters in different conditions

To further investigate whether a multi-MD-parameter can reveal more about road marking detectability than just analysing image contrast alone, $MD_{\text{Contrast, Cam}}$ and MD_{Gradient} as well as MD_{Gradient} and MD_{Edge} are compared across night/dry, night/wet, and day/dry conditions in Fig. 4(a) and (b). Specifically, Fig. 4(a) displays the quotient of $MD_{\text{Contrast, Cam}}$ and MD_{Gradient} in different conditions for flat and structured white markings. In contrast, Fig. 4(b) illustrates the quotient of MD_{Gradient} and MD_{Edge} under the same variable conditions. These figures are crucial in evaluating whether the MD parameters exhibit differences when image contrast is not the sole factor considered in the analysis.

The quotient analysis has been conducted as follows: if the parameters exhibit identical performance across different conditions, the resulting quotient will remain constant, indicating that a single parameter is sufficient to characterise MD. However, the data shows otherwise, with two observations emerging from Fig. 4(a).

- (1) The ratio of $MD_{\text{Contrast, Cam}}$ to MD_{Gradient} is higher in nighttime conditions than in daytime.
- (2) Wet conditions register a higher quotient than dry conditions during the night.

These observations lead to two conclusions from Fig. 4(a) that contribute to the conclusions drawn from Table 8 thus far. Firstly, when relying solely on contrast values and not considering the intensity gradient between road marking and road surface, the camera's detectability of road markings is overestimated during the night compared to the day. Secondly, this overestimation is more pronounced in wet conditions than in dry conditions, particularly for structured markings. Both conclusions can be explained by a difference in the sharpness of the marking edges in the camera images. The higher the quotient in Fig. 4(a), the blurrier the markings edges appear in the camera images. Relative to the contrast, the least sharp edges are found in night/wet conditions, followed by night/dry. The sharpest edges are found in daytime conditions.

Contrast is often used to measure how well camera images can detect the edges of road markings, as mentioned in Burghardt et al. (2020, 2023). However, the findings reveal that relying solely on contrast does not always work well across different conditions. This is because the detectability of a road marking edges in an image depends not just on contrast but also on how clear or blurry the edge looks. Considering that the gradient intensity of a marking's edge is not solely determined by its contrast but also by the blurriness of the edge's appearance in the image, the quality standards for image contrast required for safe detection vary significantly with changing environmental conditions analysed in this study. Following the discussion, night/wet conditions demand the highest camera contrast to realise the same gradient intensity of marking edges, succeeded by night/dry, day/dry, and day/moist conditions.

Now that the advantage of MD_{Gradient} is discussed, the benefit of MD_{Edge} is analysed next. As previously stated, MD_{Edge} provides a more comprehensive analysis by encompassing the entire road surface, whereas MD_{Gradient} concentrates exclusively on the edges of the markings. If the ratio of MD_{Edge} to MD_{Gradient} remained constant across different conditions, it would imply that the edge intensities of non-marking objects change in correlation with those of road markings, making it unnecessary to consider the wider road surface. However, the data demonstrates that this is not the case, leading to two observations from Fig. 4(b).

- (1) The ratio of MD_{Edge} to MD_{Gradient} is higher in nighttime conditions than in daytime.
- (2) This ratio is lower for flat markings when evaluated in wet conditions.

Accordingly, two conclusions can be drawn from Fig. 4(b). By solely looking at the marking and its closest surroundings rather than at the whole street, camera detectability is (1) overestimated in daytime conditions compared to nighttime conditions and (2) overestimated in wet conditions compared to dry conditions at night, especially for flat markings. Both conclusions can be explained by a varying presents of non-marking edges in the camera images. The lower the quotient in Fig. 4(b), the more a marking detection in the camera image might be distracted by false positive detection. The most distracting non-marking edges are found in daytime conditions, followed by night/wet

conditions. Hardly any non-marking edges can be found in images taken under night/dry conditions.

The common approach of assessing marking detection in images by focusing solely on the marking and its adjacent area has proven to be inadequate when environmental conditions vary. This explains why different studies show inconsistent recommendations, as highlighted in [Pike et al. \(2018a\)](#). Since detectability is contingent on factors beyond the properties of the road marking itself, the established quality standards of road markings seem to require significant adjustment to accommodate different environmental conditions and roadway surfaces.

5. Conclusions

The study investigated into the MD of road markings under varying conditions. It proposed a transparent signal processing metric to determine the MD of road markings. This metric includes a new set of MD parameters that evaluate the input quality for common feature extraction methods, such as thresholding, edge detection, and ridge detection. The following specific conclusions could be drawn.

- Research question A, which asked for correlations between MD parameters and common photometric road markings parameters, was partly verified. In nighttime conditions, R_L was proved as a reliable predictor for MD in camera images, regardless of surface wetness.
- In addition, R_L has also been found to be a good predictor for contrast in LiDAR point clouds under dry or moist conditions, during both nighttime and daytime. However, in contrast to its performance with camera-based detection, R_L is an unreliable predictor for LiDAR contrast in wet conditions; it is likely that the use of R_L measured under wet conditions would be more appropriate.
- Additionally, Q_d of road markings could not have been proven as a predictor for MD in daytime conditions, which might be explained by a saturation effect where increasing Q_d does not correspond to increased contrast in camera images. This suggests that the research into Q_d may need reevaluation, using low Q_d road markings.
- The study demonstrated that different parameters, such as contrast, gradient, and edge detectability, perform variably under diverse environmental conditions. This highlights the advantages of using multiple MD parameters to assess road marking detectability comprehensively.
- Relying solely on one parameter, like image contrast, can lead to inaccurate assessments, either overestimating or underestimating the MD of road markings. This helps explain the inconsistencies in recommendations for minimum quality levels across different studies, underscoring the need for a multi-parameter approach.
- Furthermore, the proposed multi-parameter approach provides a more consistent and realistic method for advancing research into minimum standards for road marking quality. Such approach not only facilitates the investigation of various effects and phenomena relevant to safe road marking detection, including false-positive

detections, but also offers practical implications for future research and application.

- To establish robust and demand-oriented road marking standards, it is recommended to apply the multi-parameter approach to a broader and more diverse dataset, incorporating more challenging scenarios such as curved roads with altering viewing angles and limited viewing distances; severe weather conditions, such as heavy rain, swirling spray from vehicles, fog, and snow; and the influence of adverse lighting conditions, including glare from other vehicles, low sun, and streetlights.

Ultimately, the study advocates adjusting quality standards of road markings to match specific environmental and road surface conditions, ensuring road markings are effectively detectable. For the safe integration of automated driving systems, car manufactures and road operators need to collaborate further on defining ODDs in a manner that enables demand-oriented and validated operation of roads ODs for automated vehicles. The study emphasises the necessity of situational and dynamic standards over static ones to accurately reflect the complexities of real-world driving environments and maintain consistent detectability.

Conflict of interest

The authors do not have any conflict of interest with other entities or researchers.

CRedit authorship contribution statement

Stefan Biermeier: Writing – original draft, Software, Methodology, Formal analysis, Data curation. **Dirk Kemper:** Supervision, Project administration, Investigation, Funding acquisition, Conceptualization. **Tomasz E. Burghardt:** Supervision, Resources, Methodology, Funding acquisition. **Alvaro Garcia-Hernandez:** Writing – review & editing, Writing – original draft, Visualization, Validation, Supervision, Methodology.

Declaration of generative AI and AI-assisted technologies in the writing process

During the preparation of this work, the authors used ChatGPT in order to edit the grammar of the paper. After using this tool, the authors reviewed and edited the content as needed and takes full responsibility for the content of the publication.

Acknowledgments

The authors acknowledge the German Federal Highway Research Institute (BAST) project FE 0.3.0590/2019/EGB, which

funded part of the measurements in this study. Additionally, the authors express their gratitude to SWARCO for funding the test drives with the sensor-equipped vehicle.

REFERENCES

- Amaradi, P., Sriramoju, N., Dang, L., et al., 2016. Lane following and obstacle detection techniques in autonomous driving vehicles. In: 2016 IEEE International Conference on Electro Information Technology (EIT), Grand Forks, 2016.
- Babić, D., Fiolić, M., Žilioniene, D., 2017. Evaluation of static and dynamic method for measuring retroreflection of road markings. *Gradevinar* 69 (10), 907–914.
- Babić, D., Babić, D., Fiolić, M., et al., 2021. A comparison of lane marking detection quality and view range between daytime and night-time conditions by machine vision. *Energies* 14 (15), 4666.
- Brémond, R., 2019. Visual performance models in road lighting: a historical perspective. *Leukos* 17 (3), 212–241.
- Burghardt, T.E., Chistov, O., Reiter, T., et al., 2023. Visibility of flat line and structured road markings for machine vision. *Case Studies in Construction Materials* 18, e02048.
- Burghardt, T.E., Mosböck, H., Pashkevich, A., et al., 2020. Horizontal road markings for human and machine vision. *Transportation Research Procedia* 48, 3622–3633.
- Burghardt, T.E., Pashkevich, A., Bartusiak, J., 2021. Solution for a two-year renewal cycle of structured road markings. *Drogi i Mosty* 20, 5–18.
- Burghardt, T.E., Pashkevich, A., Mosböck, H., 2019. Yellow pedestrian crossings: from innovative technology for glass beads to a new retroreflectivity regulation. *Case Studies on Transport Policy* 7 (4), 862–870.
- Burghardt, T.E., Popp, R., Helmreich, B., et al., 2021b. Visibility of various road markings for machine vision. *Case Studies in Construction Materials* 15, e00579.
- Calvi, A., 2014. A study on driving performance along horizontal curves of rural roads. *Journal of Transportation Safety & Security* 7 (3), 243–267.
- Canny, J., 1986. A computational approach to edge detection. *IEEE Transactions on Pattern Analysis and Machine Intelligence* 8 (6), 679–698.
- Carlson, P., Park, E., Kang, D., 2013. Investigation of longitudinal pavement marking retroreflectivity and safety. *Transportation Research Record* 2337, 59–66.
- Duda, R., Hart, P., 1972. Use of the Hough transformation to detect lines and curves in pictures. *Communications of the ACM* 15, 1–15.
- Fischler, M., Bolles, R., 1981. Random sample consensus: a paradigm for model fitting with applications to image analysis and automated cartography. *Communications of the ACM* 24 (6), 381–395.
- Haloi, M., Jayagopi, D., 2015. A robust lane detection and departure warning system. *IEEE Intelligent Vehicles Symposium (IV)*, 126–131.
- Han, L., Du, Z., Zheng, H., et al., 2023. Reviews and prospects of human factors research on curve driving. *Journal of Traffic and Transportation Engineering (English Edition)* 10 (5), 808–834.
- Huang, J., Liang, H., Wang, Z., et al., 2013. Robust lane marking detection under different road conditions. In: 2013 IEEE International Conference on Robotics and Biomimetics (ROBIO), Shenzhen, 2013.
- Kanopoulos, N., Vasanthavada, N., Baker, R., 1988. Design of an image edge detection filter using the Sobel operator. *IEEE Journal of Solid-State Circuits* 23 (2), 358–367.
- Katzorke, N., Kastner, S., Kolar, P., et al., 2022. Agile altering of road marking patterns for lane detection testing. *IEEE Transactions on Intelligent Transportation Systems* 23 (11), 21996–22001.
- Kim, K.-W., Im, J.-H., Heo, M.-B., et al., 2019. Precise vehicle position and heading estimation using a binary road marking map. *Journal of Sensors*, <https://doi.org/10.1155/2019/1296175>.
- Li, H., Tarik, K., Arefnezhad, S., et al., 2021. Phenomenological modelling of camera performance for road marking detection. *Energies* 15 (1), 194.
- Lim, K.L., Braunl, T., 2019. A methodological review of visual road recognition procedures for autonomous vehicle applications. *arXiv*, 1905.01635.
- Muckenhuber, S., Softic, K., Fuchs, A., et al., 2021. Sensors for automated driving. In: Van Uytsel, S., Vasconcellos Vargas, D. (Eds.), *Perspectives in Law, Business and Innovation*. Springer, Singapore, pp. 115–146.
- Marr, J., Benjamin, S., Zhang, A., 2020. Implications of Pavement Markings for Machine Vision. *Austroads Project FPI6119*. Austroads, Sydney.
- O'Mahony, N., Campbell, S., Carvalho, A., et al., 2019. Deep learning vs. traditional computer vision. In: *Advances in Computer Vision (CVC 2019)*, Las Vegas, 2019.
- Otsu, N., 1979. A threshold selection method from gray-level histograms. *IEEE Transactions on Systems, Man, and Cybernetics* 9 (1), 62–66.
- Pappalardo, G., Cafiso, S., Di Graziano, A., et al., 2021. Decision tree method to analyze the performance of lane support systems. *Sustainability* 13 (2), 846.
- Pappalardo, G., Caponetto, R., Varrica, R., et al., 2022. Assessing the operational design domain of lane support systems for automated vehicles in different weather and road conditions. *Journal of Traffic and Transportation Engineering (English Edition)* 9 (4), 631–644.
- Pike, A., Barrette, T., Carlson, P., 2018a. Evaluation of the Effects of Pavement Marking Characteristics on Detectability by ADAS Machine Vision. Project No. 20-102 (06). Texas A&M University, College Station.
- Pike, A., Barrette, T., Carlson, P., 2018b. Evaluation of the Effects of Pavement Marking Width on Detectability by Machine Vision: 4-inch vs 6-inch Markings. Texas A&M Transportation Institute, College Station.
- Pike, A., Whitney, J., Hedblom, T., et al., 2019. How might wet retroreflective pavement markings enable more robust machine vision? *Transportation Research Record* 2673, 361–366.
- Pocock, B.W., Rhodes, C.C., 1952. Principles of glass-bead reflectorization. *Highway Research Board* 57, 32–48.
- Saint-Jacques, E., Brémond, R., 2023. Wet road surfaces, a challenge for road users... and for measurement. In: Ullis, L. (Ed.), *Radiometry of Wet Surfaces*. EDP Sciences, Paris, pp. 63–72.
- Schnell, T., Aktan, F., Lee, Y., 2003. Nighttime visibility and retroreflectance of pavement markings in dry, wet, and rainy conditions. *Transportation Research Record* 1824, 144–155.
- Storsæter, A., Pitera, K., McCormack, E., 2021a. Using ADAS to future-proof roads-comparison of fog line detection from an in-vehicle camera and mobile retroreflectometer. *Sensors* 21, 1737.
- Storsæter, A., Pitera, K., McCormack, E., 2021b. Camera-based lane detection—can yellow road markings facilitate automated driving in snow? *Sensors* 4, 661–690.
- Veit, T., Tarel, J., Nicolle, P., et al., 2008. Evaluation of road marking feature extraction. In: 11th International IEEE

Conference on Intelligent Transportation Systems, Beijing, 2008.

Wenzel, K., Burghardt, T.E., Pashkevich, A., et al., 2022. Glass beads for road markings: surface damage and retroreflection decay study. *Applied Science* 12 (4), 2258.

Yang, M., Bao, Q., Shen, Y., et al., 2023. Thirty years of research on driving behavior active intervention: a bibliometric overview. *Journal of Traffic and Transportation Engineering (English Edition)* 10 (5), 721–742.

Yeong, D., Velasco-Hernandez, G., Barry, J., et al., 2021. Sensor and sensor fusion technology in autonomous vehicles: a review. *Sensors* 21, 2140.



Stefan Biermeier received the MSc degree in civil engineering from RWTH Aachen University in 2020, where he is currently pursuing the PhD degree. From 2019 to 2023, he was a researcher in the field of traffic engineering and since 2024, he has been heading the Research Group of Management of Roadside Equipment at the Institute of Highway Engineering, RWTH Aachen University. His research interests include road markings, autonomous driving, and road

maintenance management systems.



Tomasz E. Burghardt earned his doctorate from Purdue University in 2005 and defended his habilitation in the discipline of civil engineering, geodesy, and transportation at Kraków University of Technology in 2024. His work experience includes development of coatings and research on sizing for glass. Since 2010 employed at SWARCO, as research and development project manager, he has been working on various topics associated with road markings, currently on their environmental assessment and visibility.



Alvaro Garcia-Hernandez received his doctorate in engineering from the University of Cantabria, Spain. He is a professor at RWTH Aachen University, where he leads the Institute of Highway Engineering. With extensive expertise in pavement engineering, his research focuses on sustainable road materials, including cold in-situ recycling, self-healing materials, biobitumen applications, and pavement durability modelling.